Submitted to Physical Review Letters

LBL-2032
Preprint c.1

NONLINEAR ATTENUATION OF AN ELECTROMAGNETIC BEAM BY SIDE- AND BACK-SCATTERING IN AN INHOMOGENEOUS PLASMA

Michael A. Mostrom, Dwight R. Nicholson,
and Allan N. Kaufman

May 31, 1973

For Reference

Not to be taken from this room

Prepared for the U.S. Atomic Energy Commission
under Contract W-7405-ENG-48

DISCLAIMER

This document was prepared as an account of work sponsored by the United States Government. While this document is believed to contain correct information, neither the United States Government nor any agency thereof, nor the Regents of the University of California, nor any of their employees, makes any warranty, express or implied, or assumes any legal responsibility for the accuracy, completeness, or usefulness of any information, apparatus, product, or process disclosed, or represents that its use would not infringe privately owned rights. Reference herein to any specific commercial product, process, or service by its trade name, trademark, manufacturer, or otherwise, does not necessarily constitute or imply its endorsement, recommendation, or favoring by the United States Government or any agency thereof, or the Regents of the University of California. The views and opinions of authors expressed herein do not necessarily state or reflect those of the United States Government or any agency thereof or the Regents of the University of California.

NONLINEAR ATTENUATION OF AN ELECTROMAGNETIC BEAM BY SIDE- AND BACK-SCATTERING IN AN INHOMOGENEOUS PLASMA*

Michael A. Mostrom, Dwight R. Nicholson, and Allan N. Kaufman

Department of Physics and Lawrence Berkeley Laboratory
University of California, Berkeley, California 94720

May 31, 1973

ABSTRACT

The theory of nonlinear attenuation is developed for an intense laser beam of diameter D, propagating into an inhomogeneous plasma of density scale-length L. The attenuation results from the exponential growth of electromagnetic noise, due to parametric Raman instability, with local excitation of plasma waves at frequency ω_p and damping rate ν_p. The scattered waves are predominantly sideways or backwards, depending on the ratio $(\nu_p/\omega_p)(L/D)$. Threshold intensities for effective extinction are calculated.

There has been much recent interest in parametric Raman instability (induced decay of an electromagnetic wave into another electromagnetic wave and an electron plasma wave), because it may prevent laser energy from reaching the denser regions of a pellet plasma. Among several studies of parametric instability in an inhomogeneous plasma,[1-3] the Raman instability has been treated one-dimensionally by Liu and Rosenbluth,[4] who derived a threshold for significant back-scatter, and by Forslund et al.,[5] who studied nonlinear aspects analytically and by numerical simulation. Here we present a three-dimensional

treatment,[6] allowing for scattering in all directions. We show that side-scattering may greatly exceed back-scattering. We calculate its angular spread, and derive the nonlinear attenuation of the incident beam, and the thresholds for significant extinction due to either side- or back-scattering.

Our model is an intense plane-polarized electromagnetic beam, of frequency ω_0 and wave vector $\vec{k}_0 = k_0 \hat{z}$, and with uniform intensity over its circular cross section of diameter D, incident on a cold underdense plasma in the direction of the density gradient (see Fig. 1). The polarization $\hat{e}_0$ is along x; the slight z-field,[7] due to finite D, is ignored. The intensity is assumed to be below the absolute instability threshold;[8-10] this requires $\omega_p < \frac{1}{2}\omega_0$, and allows us to study steady-state solutions. We further assume that the laser pulse is sufficiently short to prevent the buildup of a radial density gradient from Brillouin scattering[4,5] or filamentation.[11] The effect of finite temperature on the plasma wave is discussed later.

For a scattered wave $\vec{k}_1$, $\omega_1 \equiv [k_1^2c^2 + \omega_p^2(z)]^{1/2}$, growing from thermal noise, the local driven longitudinal mode has $\vec{K} \equiv \vec{k}_0 - \vec{k}_1$, $\Omega \equiv \omega_0 - \omega_1$; the parametric growth rate is largest in the resonant region $\omega_p(z) \approx \Omega$. As there is a spectrum of waves at each point, we express the total vector and scalar potentials as

$$\vec{A}(\vec{x},t) = \hat{e}_0 A_0(\vec{x}) \exp i(\vec{k}_0\cdot\vec{x} - \omega_0 t) + \sum_{\vec{k}_1} \hat{e}_1 A(\vec{k}_1,\vec{x}) \exp i(\vec{k}_1\cdot\vec{x} - \omega_1 t) + \text{c.c.},$$

$$\phi(\vec{x},t) = -i \sum_{\vec{k}_1} \phi(\vec{K},\vec{x}) \exp i(\vec{K}\cdot\vec{x} - \Omega t) + \text{c.c.}\ .$$

The slowly varying amplitudes are defined over a Fourier box length $\ell \ll D$. We ignore WKB effects on the amplitudes, valid for $\omega_p < \frac{1}{2}\omega_0$.

The evolution of the amplitudes is obtained[12] from a Lagrangian description, yielding a straightforward three-dimensional generalization of the equations of Cohen et al.:[13]

$$\left[(\partial/\partial t) + \nu_p - i\Delta(k_1,z)\right]\phi(\vec{K},\vec{x}) = (e\omega_p\, \hat{e}_0\cdot\hat{e}_1/2mc^2)A_0(\vec{x})A^*(\vec{k}_1,\vec{x}), \qquad (1a)$$

$$\left[(\partial/\partial t) + \nu_1 + \vec{c}_1\cdot\nabla\right]A(\vec{k}_1,\vec{x}) = (e\, K^2\, \hat{e}_0\cdot\hat{e}_1/2m\omega_1)A_0(\vec{x})\phi^*(\vec{K},\vec{x}); \qquad (1b)$$

where $\Delta \equiv \Omega(k_1) - \omega_p(z)$ is the frequency mismatch, $\vec{c}_1 \equiv \vec{k}_1\, c^2/\omega_1$ is the group velocity, and the damping rates ν_p, ν_1 have been introduced phenomenologically. Ignoring transients, and solving for the steady state, we eliminate ϕ to obtain

$$(\nu_1 + \vec{c}_1\cdot\nabla)A(\vec{k}_1,\vec{x}) = \alpha|a_0|^2\, \omega_0\omega_p(\nu_p + i\Delta)^{-1}\, A(\vec{k}_1,\vec{x}),$$

where $a_0 \equiv e\, A_0/mc^2$ and $\alpha \equiv (\hat{e}_0\cdot\hat{e}_1)^2\, K^2c^2/(4\omega_0\omega_1) \sim 1$. Multiplying by A^* and adding the complex conjugate yields the convection equation:

$$\vec{c}_1\cdot\nabla|A(\vec{k}_1,\vec{x})|^2 = 2\gamma_1(\vec{k}_1,\vec{x})\,|A(\vec{k}_1,\vec{x})|^2 + 2\nu_1\,|A(\vec{k}_1)|^2_{th}\,, \qquad (2)$$

where $\gamma_1 \equiv \alpha|a_0|^2\, \omega_0\omega_p(\nu_p^2 + \Delta^2)^{-1} - \nu_1$ is the local growth rate of the convective instability, and a thermal source term has been added. Integration of (2), along a ray path from a source point s_0 outside the beam to the exit point s_1 at $\vec{x}$, yields[14]

$$|A(\vec{k}_1,\vec{x})|^2 = |A(\vec{k}_1)|^2_{th}\, \exp\Gamma(\vec{k}_1,\vec{x}),$$

where the exponentiation integral is $\Gamma(\vec{k}_1,\vec{x}) \equiv 2\int_{s_0}^{s_1} \gamma_1(s)ds/c_1$.

The dependence of γ_1 on Δ limits the effective region of growth to a cylindrical resonance region (see Fig. 1) of diameter D, centered at $\Delta(k_1,z') = 0$ [which defines $z'(k_1)$], and of height $h \equiv 4\pi(\nu_p/\omega_p)L$ [defined so that $\Delta < 2\pi\,\nu_p$], where $L \equiv (d\,\ell n\, n/dz)^{-1}$ is the density scale length. Explicit calculation of Γ for side-scattering ($\vec{k}_1 = \pm\, k_1\hat{y}$, $K \approx \sqrt{2}\, k_0$) yields

$\Gamma_S \equiv \frac{1}{2}\, |a_0|^2(\omega_p/\nu_p)(K^2D/k_1)$, while for back-scattering[4] ($\vec{k}_1 = -k_1\hat{z}$, $K \approx 2\, k_0$) we obtain $\Gamma_B \equiv \pi|a_0|^2(K^2L/k_1)$. Their ratio is $\Gamma_S/\Gamma_B = (D/h)[2(k_0^2 + k_1^2)/(k_0 + k_1)^2] \approx D/h$. Hence the relative predominance of scattering sideways and backwards is given by the relative dimensions of the resonance zone.

A detailed study[12] of side-scattering, under conditions that it predominates ($D/h > 2$, $\Gamma_S > 10$), indicates that the scattered radiation is highly collimated: the exponentiation $\Gamma(\vec{k}_1,\vec{x})$ is appreciable for $\vec{k}_1$ lying in an elliptical cone about $\pm\,\hat{y}$, with polar half-angle $(h/4D)\Gamma_S^{-1/2}$ and azimuthal half-angle $\Gamma_S^{-1/2}$.

Upon integrating the scattered radiation intensity over the surface of the beam,[12] energy conservation (with allowance for the fraction ω_p/ω_0 deposited in the plasma)[13] can be used to determine the attenuation coefficient $\kappa(z) \equiv -\, d\,\ell n\, I/dz$ of the incident intensity $I(z)$. For side-scattering the result can be expressed as

$$\kappa_S L = \exp(\Gamma_S - G_S)\,, \qquad (3)$$

where G_S is the solution of the transcendental equation

$$G_S = \ell n[(mc^2/T)(D/r_e)(\omega_0/\nu_p)(k_0L)^{-2}\, g_S] + 3\,\ell n\, G_S\,,$$

where T is the electron temperature (providing the thermal source of noise: $|A(\vec{k}_1)|^2_{th} = 2\pi c^2T/\ell^3\omega_1^2$), $r_e \equiv e^2/mc^2$, and $g_S(\omega_p/\omega_0) \approx 1$ for $\omega_p < \omega_0/2$. For typical values (see Table 1), G_S lies between 30 and 40. Noting that Γ_S is proportional to the intensity I, we see from (3) that κ_S is a rapidly increasing function of I. We

define the threshold intensity I_S by setting $\kappa_S = L^{-1}$, whence $\Gamma_S = G_S$ at threshold, or $I_S = G_S(v_p/\omega_p)(mc^3/r_e\lambda_0 D)f$, with $\lambda_0 \equiv 2\pi/k_0$ and $f(\omega_p/\omega_0) \approx 1$ for $\omega_p < \omega_0/2$. In units of 10^{12} W/cm^2,

$I_S = 90\, G_S(v_p/\omega_p)(\omega_0/\omega_{CO_2})D_{mm}^{-1}$.

An approximate analysis[15] of back-scattering, under conditions that it predominates ($D < h$, $\Gamma_B > 10$), yields the corresponding attenuation coefficient

$$\kappa_B L = \exp(\Gamma_B - G_B) , \qquad (3_B)$$

with G_B the solution of

$G_B = \ln[(mc^2/T)(L/r_e)(v_p/\omega_p)^2(\omega_0/\omega_p)(k_0 D)^{-2}\, g_B] + \ln G_B$,

where $g_B \sim (4\pi)^3$ for $\omega_p/\omega_0 < \frac{1}{2}$. For typical values, G_B lies between 25 and 35. Accordingly, the threshold intensity for predominant back-scattering is, in units of 10^{12} W/cm^2,

$I_B = 7\, G_B(\omega_0/\omega_{CO_2})L_{mm}^{-1}$. This threshold is a factor $G_B/2\pi$ higher than the one-dimensional result[4] of Liu and Rosenbluth, since their criterion of significant attentuation was $\Gamma_B = 2\pi$.

In the previous calculations we have used a cold plasma model; finite temperature effects can be studied by including the convection term $(3\, v_e^2/\Omega)\vec{K} \cdot \nabla \phi(\vec{K},\vec{x})$ on the left of (1a). The equations can again be solved (for $\Gamma \gg 1$) with the main finite temperature modification[12] being a small increase (less than a factor of 2) in the local growth rate γ_1 (and a proportionate decrease in threshold) provided that

$$X \equiv 12\, \alpha\, |a_0|^2 (v_e^2/c^2)(\omega_0^2/v_p^2)(K^2/2k_0^2) < 1.$$

Calculations in a homogeneous medium indicate that the instability

becomes absolute for $X > 1$; then our steady state assumption breaks down. For example (II) in Table 1, $X = 0.64$ at threshold.

We thank C. S. Liu for his initial inspiration, and B. Cohen and C. Max for many helpful discussions.

FOOTNOTES AND REFERENCES

* Work supported by the U. S. Atomic Energy Commission, and by NDEA Title IV (MM), and National Science Foundation (DN), and the Air Force Office of Scientific Research (AK).

1. T. Amano and M. Okamoto, J. Phys. Soc. Japan 26, 529 (1969).
2. M. Rosenbluth, Phys. Rev. Letters 29, 565 (1972).
3. F. Perkins and J. Flick, Phys. Fluids 14, 2012 (1972).
4. C. S. Liu and M. Rosenbluth, Institute for Advanced Study preprint C003237-11.
5. D. Forslund, J. Kindel, and E. Lindman, Phys. Rev. Letters 30, 739 (1973).
6. A preliminary version of this work was reported in Bull. Am. Phys. Soc. 17, 1065 (1972).
7. C. Vittitoe and T. Wright, Phys. Rev. Lett. 30, 1025 (1973).
8. J. Kindel (private communication).
9. D. DuBois and E. Williams. University of Colorado preprint CU-1005.
10. B. Fried, G. Schmidt, and R. Gould, University of California at Los Angeles preprint PPG-146.
11. P. Kaw, G. Schmidt, and T. Wilcox, Phys. Fluids (in press).
12. M. Mostrom, Lawrence Berkeley Laboratory report (unpublished).
13. B. Cohen, A. Kaufman, and K. Watson, Phys. Rev. Letters 29, 581 (1972).

14. A term vanishing as $\nu_1 \to 0$ is omitted.

15. D. Nicholson, Lawrence Berkeley Laboratory report (unpublished).

Table 1

	n (cc^{-1})	T (eV)	ν_p/ω_p	L (mm)	h (mm)	D (mm)	ω_0 (sec^{-1})	ω_0/ω_p	G_S	I_S (W/cm^2)
I	10^{17}	30	10^{-3}	10^2	1.2	3	2×10^{14}	10	35	9×10^{11}
II	10^{20}	10^3	10^{-2}	0.1	0.012	0.1	2×10^{15}	3	37	3×10^{15}

CAPTIONS

Table 1. Thresholds for typical parameters. (I) Theta pinch, CO_2 laser. (II) Laser-pellet fusion experiment, Nd: glass laser. In both examples, $D > h$; so side-scattering predominates.

Figure 1. Resonance zone geometry. The laser beam diameter is D. The center of the resonance zone is at $z'(k_1)$; its height is $h \equiv 4\pi(v_p/\omega_p)L$.

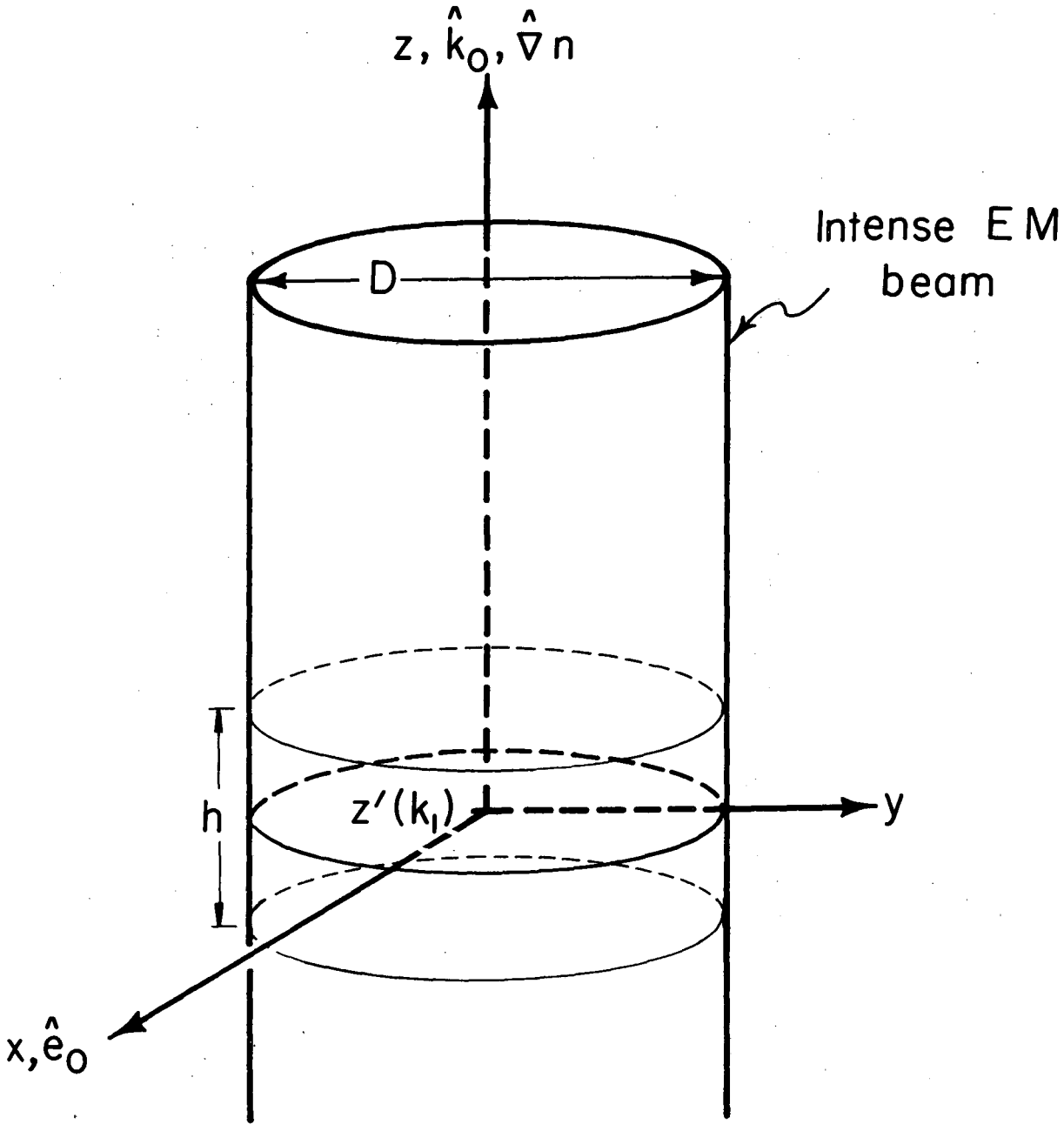

XBL735-2975

Fig. 1

LEGAL NOTICE

This report was prepared as an account of work sponsored by the United States Government. Neither the United States nor the United States Atomic Energy Commission, nor any of their employees, nor any of their contractors, subcontractors, or their employees, makes any warranty, express or implied, or assumes any legal liability or responsibility for the accuracy, completeness or usefulness of any information, apparatus, product or process disclosed, or represents that its use would not infringe privately owned rights.

TECHNICAL INFORMATION DIVISION
LAWRENCE BERKELEY LABORATORY
UNIVERSITY OF CALIFORNIA
BERKELEY, CALIFORNIA 94720